ISSN 0005-1179 (print), ISSN 1608-3032 (online), Automation and Remote Control, 2023, Vol. 84, No. 10, pp. 1232–1242.

TOPICAL ISSUE

Information Support for Aircraft Crew in Takeoff and Landing Modes

A. M. Shevchenko[*,a], **B. V. Pavlov**[*,b], **and G. N. Nachinkina**[*,a]

[*] *Trapeznikov Institute of Control Sciences, Russian Academy of Sciences, Moscow, Russia*
e-mail: [a] *shev-chik@yandex.ru,* [b] *pavlov@ipu.ru,* [c] *nach_gala@ipu.ru*

Received June 19, 2023
Revised July 28, 2023
Accepted August 2, 2023

Abstract—Methods for assessing the current state and forecasting critical events are developed in order to reduce the stress load on the pilot of an aircraft. These methods are based on the energy approach to flight control. Algorithms for forecasting the possibility of safe takeoff in the presence of high-rise obstacles on the trajectory are obtained. Forecast correction algorithms are introduced. Algorithms for calculating the braking distance depending on the runway condition are found in the modes of landing or emergency braking at takeoff. Some ways to correct forecasts considering the sequence and operation time of all braking devices are proposed. Model tests are carried out for the algorithms in the entire range of operating conditions.

Keywords: takeoff, landing, forecasting methods, information support, energy approach

DOI: 10.25728/arcRAS.2023.18.69.001

1. INTRODUCTION

The issues of organizing passenger transportation have recently become more and more acute and topical. The main directions of transportation improvement are traffic intensification and the expansion of permitted weather conditions for aircraft flights. Therefore, the safety of aviation equipment comes to the forefront.

Technical and communications progress in all spheres of human activity tends to accelerate. This progress is manifested by the increase in transportation traffic and the expansion of acceptable atmospheric or climatic conditions.

According to statistical data of the Main Center for Information Technologies and Meteorological Services for Aviation (Aviamettelecom) of the Federal Service for Hydrometeorology and Environmental Monitoring (Roshydromet) [1], there were nine aviation accidents during January–March 2023, including:

(1) three fatal accidents, particularly three fatal accidents in G-class airspace, with a death toll of 5;
(2) one non-fatal accident, including one non-fatal accident in G-class airspace;
(3) two aviation incidents in total (one aircraft landing below the operational minimum and one aircraft struck by atmospheric electricity);
(4) two industrial events (emergency events);
(5) one emergency situation without investigation (one aircraft struck by atmospheric electricity).

In a statistical study of aviation accidents on passenger flights throughout the world, Boeing demonstrated that more than half of all accidents occur during takeoff and landing stages [2]. Flight control at these stages is carried out with the direct participation of the pilot, who undergoes strong

psychological stress. Therefore, the human factor becomes governing. The statistics of aviation accidents based on the recent studies [3–5] shows that the share of aviation accidents caused by human participation in flight task fulfillment varies from 50 to 70% depending on the estimation methods.

One safety improvement direction is to equip aircraft with onboard systems providing instrument-based control of critical motion coordinates during two stages: ground run on the runway during landing and takeoff. Information support for the pilot and the creation of a pilot-friendly interaction environment with cockpit equipment have become necessary. For this purpose, forecasting methods and new algorithms [6–8] were developed to calculate the aircraft motion on the ground segment of the trajectory.

In particular, it was decided to supplement onboard equipment with an information measuring system (IMS) of takeoff run control [6]. This system simultaneously monitors longitudinal acceleration, speed, and distance to reach the target speed. The forecasted distance to the decision point helps the pilot to make a timely decision. But if the forecasted distance differs from the standard one by an unacceptable value, the IMS generates a signal to alert the pilot and a command signal to prohibit takeoff. In [7, 8], some variants of safe forecasted takeoff and emergency braking in unfavorable climatic conditions and geographical coordinates were developed. These solutions are conceptually based on the energy approach to controlling the spatial motion of an aircraft, first presented in [9].

This paper further refines methods for assessing the current situation and forecasting the aircraft's motion on the runway in the braking modes after landing or aborted takeoff and in the ground run stage before takeoff. In addition, we develop methods for increasing situational awareness to eliminate stress load and reduce the risks of erroneous actions of the pilot.

2. THE ENERGY BALANCE EQUATION FOR AIRCRAFT MOTION

Historically, the basic controllable coordinates of an aircraft are altitude, speed, and the direction of flight. They are natural for flight control both in visual orientation mode and in instrument flight. The theory and practice of automatic control were developed in the same line. The concept of flight control in the longitudinal channel of the aircraft using two loops—trajectory and speed—became established in aviation. In automatic flight control systems, the functions of controllers are performed by independent devices, namely, thrust automaton and autopilot. Controller design problems with classical methods neglect the nonlinear relationship between the two main variables (speed and flight altitude), which is provided by the fundamental law of conservation of energy of a body moving in a potential field of forces.

In contrast to the conventional description of the spatial motion of an aircraft by the Cauchy equations, the paper [10] proposed a control concept with the total energy of motion

$$E = mgh + \frac{mV^2}{2},$$

where m denotes the weight of the aircraft, h is the flight altitude, and V is the speed in the inertial frame.

We will consider motion in terms of the weight-normalized specific energy of motion H_E, which is also called the pseudo-energy or energy height:

$$H_E = \frac{E}{mg} = h + \frac{V^2}{2g}.$$

Being jointly solved, the dynamic equations of translational motion in the disturbed atmosphere and the total energy equation of an object yield the **energy balance equation**

$$\Delta H_E = \Delta H_E^{\text{eng}} + \Delta H_E^D + \Delta H_E^{gear} + \Delta H_E^w.$$

This equation describes quantitative relations between the energy source and all its consumers in the "aircraft–engine–environment" system. The equation is written in increments and contains the following terms: ΔH_E is the increment of the energy height of the aircraft; ΔH_E^{eng} is the specific work of the engine; ΔH_E^D is energy costs to overcome the aerodynamic drag; ΔH_E^{gear} is energy costs to overcome the resistance of landing gear; finally, ΔH_E^w is wind work. For each term, the following expressions were derived in [8, 9]: $\Delta H_E = \int_{t_1}^{t_2} V_B(\theta + \frac{\dot V_B}{g})dt$, where V_B is airspeed and θ is the angle of inclination of the trajectory in the inertial frame; $\Delta H_E^{eng} = \int_{t_1}^{t_2} V_B P_H \cos(\alpha_B + \phi_{eng})dt$, where $P_H = \frac{P}{mg}$ is the normalized thrust, α_B is the angle of attack, and ϕ_{eng} is the angle of engine installation; $\Delta H_E^D = \int_{t_1}^{t_2} V_B D_H dt$, where $D_H = \frac{D}{mg}$ is the normalized drag; $\Delta H_E^w = \int_{t_1}^{t_2} V_B f_w dt$, where the factor $f_w \approx \frac{\dot w_x}{g} - \frac{\dot w_y}{V_B}$ is called the wind factor or hazard index, and w_x and w_y are the projections of wind speed on the inertial frame axes; finally, $\Delta H_E^{gear} = \int_{t_1}^{t_2} V k_{brak} f_w dt$, where k_{brak} is the generalized normalized braking coefficient (the total resistive force of landing gear divided by aircraft weight).

3. BASIC ALGORITHMS OF ENERGY CONTROL SYSTEM

The energy height H_E has two components characterizing potential and kinetic energies, respectively. When moving in space, each component changes not independently but in according with the law of conservation of total energy. Therefore, the problem of designing flight control algorithms is naturally posed as a problem of multicriteria control. The first criterion is to minimize the deviation of the energy height: $\Delta H \to \min$. The second criterion is to minimize the mismatch between its kinetic and potential components:

$$\Delta H_E^{kin} - \Delta H_E^{pot} \to \min.$$

In the energy control system (EnCS), the thrust P is the only control variable affecting the total energy of the aircraft; the elevating rudder deviation δ_B causes a redistribution of the potential and kinetic components.

The forces in projections on the axes of the air frame satisfy the equation

$$m\dot V_B = P\cos(\alpha_B + \phi_{eng}) - D - mg\sin\theta_B - m(\dot W_{xg}\cos\theta_B + \dot W_{yg}\sin\theta_B),$$

where V_B is airspeed, α_B is the angle of attack in the air frame, D is drag, θ_B is the trajectory's angle of inclination in the air frame, and W_{xg} and W_{yg} are the projections of wind speed on the axes of the Earth frame. Resolving this equation for P under the assumption of small angles and passing to the normalized variables, we obtain

$$P_H = \theta + \frac{\dot V_B}{g} + f_w + D_H.$$

In the steady-state flight mode without wind, the simplified thrust control law in the EnCS in increments relative to the set values is given by

$$\Delta P_H^{EnCS} = \Delta\theta + \frac{\Delta\dot V_B}{g}.$$

Elevating rudder control is used to minimize the mismatch between the potential and kinetic components, which does not affect the first criterion:

$$\Delta\delta_H^{EnCS} = \Delta\theta - \frac{\Delta\dot{V}_B}{g}.$$

Integral terms are added to the proportional ones to ensure astatism for the controlled coordinates.

Flight control with EnCS naturally considers the mutual influence of the speed and trajectory channels; thus, correction loops for these relationships are not needed.

4. ENERGY FORECASTING METHOD FOR TAKEOFF AND OBSTACLE CLEARANCE

The pilot's goal in the takeoff stage is to overcome a high-rise obstacle at a speed at least equal to that of stable horizontal flight. In complicated conditions, the pilot needs to assess a priori the aircraft's ability to accelerate to the takeoff speed within the runway and climb sufficiently to overcome high-rise obstacles on the takeoff course. The takeoff diagram is shown in Fig. 1.

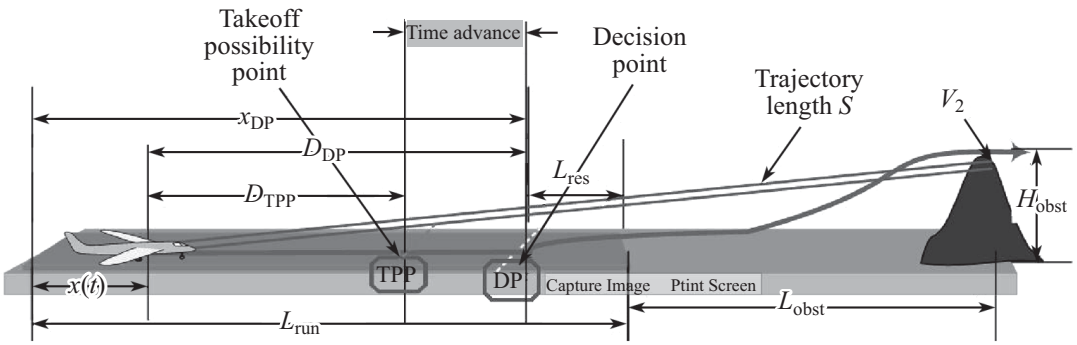

Fig. 1. Characteristic points on the takeoff trajectory.

This figure has the following notations: $x(t)$ is the current coordinate of the aircraft; H_{obst} and L_{obst} are the obstacle height and the distance to the obstacle from the runway endpoint, respectively; V_2 is the minimum speed of stable horizontal flight; S is the energy accumulation distance; L_{run} is the runway length; D_{TPP} is the distance to the takeoff possibility point (TPP); D_{DP} is the distance to the decision point (DP); x_{DP} is the coordinate of the decision point; finally, L_{res} is the takeoff run reserve from the DP to the runway endpoint.

According to the Flight Manual, takeoff is authorized when sequentially reaching the minimum horizontal flight speed V_1 and the nosewheel lift-off speed V_r regardless of the aircraft's position on the runway. However, this takeoff procedure does not ensure overcoming an obstacle safely since the speed V_r may be reached at a point in unacceptable proximity to the runway endpoint or even beyond it.

Let us inform the pilot about the possibility of a safe takeoff ahead of time by forecasting the energy state of the aircraft corresponding to the required generalized coordinates at the obstacle clearance point.

To overcome the obstacle safely, the aircraft must have a speed not less than its stable horizontal flight speed V_2. At the instant of overcoming the obstacle, the total energy $E_{H_{obst}}$ of the aircraft must contain the required minimum kinetic component and a reserve of the potential component, which gives the aircraft the necessary altitude H_{obst} for obstacle clearance:

$$E_{H_{obst}} = m\frac{V_2^2}{2} + mgH_{obst}. \tag{1}$$

The total accumulated energy of the aircraft consists of the current kinetic and potential components and the work of all external forces F_i on the trajectory of length S. Then the forecasted accumulated energy is given by

$$E(t)_{fore} = m\frac{V(t)^2}{2} + mgh(t) + S\sum_i F_i(t), \tag{2}$$

where $\sum_i F_i(t)$ is the resultant of all external forces: engine thrust, aerodynamic drag, wind force, and landing gear braking force. Equation (2) explicitly relates the energy state of the controlled object and the trajectory length to reach this state.

The resultant is naturally calculated through the longitudinal overload:

$$\sum_i F_i(t) = mgn_x(t). \tag{3}$$

Let all forces in (3) be measured during the ground run before takeoff. Equating the required (1) and forecasted (2) energies, we find the length of the forward section of the ground segment to the DP necessary to accumulate the deficient total energy:

$$D_{DP} = \frac{(g(H_{obst} - h(t)) + 0.5(V_2^2 - V(t)^2))}{gn_x(t)} - L_{obst}.$$

Note that this expression is invariant with respect to weight. The trajectory point where the forecasted length of this section becomes zero is the DP of safe takeoff: $X_{DP} = x(t)|_{D=0}$. The coordinate of this point is simply calculated as

$$X_{DP}(t) = x(t) + D_{DP}(t).$$

Total energy forecasting indicates the possibility of takeoff not at the instant of reaching the decision speed but earlier and in the distance coordinates associated with the runway.

The forecasting method based on the energy approach yields a forecast of another characteristic point on the takeoff run trajectory. Each type of aircraft is allowed to lift the front landing gear strut when reaching a known minimum takeoff run speed V_r. In abnormal situations, the pilot must assess the possibility of continuing the takeoff run and, moreover, the position of the aircraft on the runway in which it is possible to start lifting the front strut. The distance from the current position of the aircraft to reaching the rate of climb is calculated as

$$D_{V_r}(t) = \frac{V_r^2 - V^2(t)}{2gn(t)}.$$

When this forecasted distance reaches zero, it is possible to lift the front landing gear strut to turn the airplane to the takeoff angle of attack. In the course of the takeoff run, it is proposed to inform the pilot about the distance to the front strut lift point. The instrumental estimate of this distance, unlike the intuitive one, improves the pilot's situational awareness and reduces the prerequisites for erroneous actions. The distance to the front strut lift point can be shown on the instrument panel or on the display.

Situational awareness can be increased (and stress load can be reduced) when using the forecasted distance reserve to the runway endpoint at the DP:

$$L_{res}(t) = L_{run} - x(t) - D_{DP}(t).$$

A very fruitful feature of the energy method is that the current forecast considers the total energy acquired by the aircraft on the forward air segment outside the ground one. As a result, it is

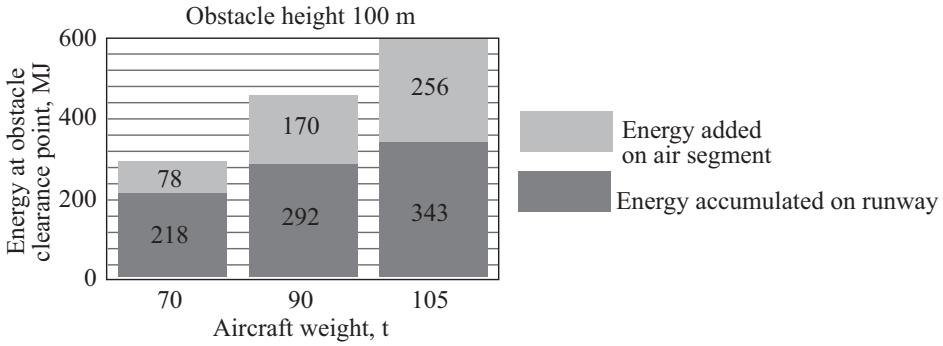

Fig. 2. Energy accumulation on the ground and air segments of the trajectory.

possible to calculate forecast values ahead of current events. Figure 2 demonstrates the energies on the ground and air segments for aircraft with three takeoff weights.

Thus, energy forecasting allows calculating the distances to all regulation events on the trajectory of a complicated takeoff ahead of time. Information about the occurrence of these events can be presented to the pilot on the cockpit indicator in text, audio, or graphic form. The pilot's awareness of the current and forecasted situation reduces the stress load and the probability of erroneous or untimely response of the pilot.

5. SIMULATION OF TAKEOFF IN THE PRESENCE OF OBSTACLES

The method for forecasting flight parameters at an obstacle clearance point was tested on a computerized bench. The bench included a complete certified model of the TU-204 aircraft, particularly the engine model and the landing gear model.

The operator's console was used to set the aircraft weight and alignment, climatic conditions, and airfield altitude and to prepare a takeoff scenario in accordance with the current flight regulations. In the bench, control during the ground run and takeoff was performed by the automatic EnCS.

The energy system saves and efficiently utilizes the resources of the controls—throttle lever and altitude channel knob—for spatial maneuvering. Therefore, the takeoff scenario contained only the required speed and altitude values.

Figure 3 shows the transients in the height YG and speed VP at takeoff in the presence of a 100 m-high obstacle at a distance of 1000 m from the runway endpoint for an aircraft with three different takeoff weights.

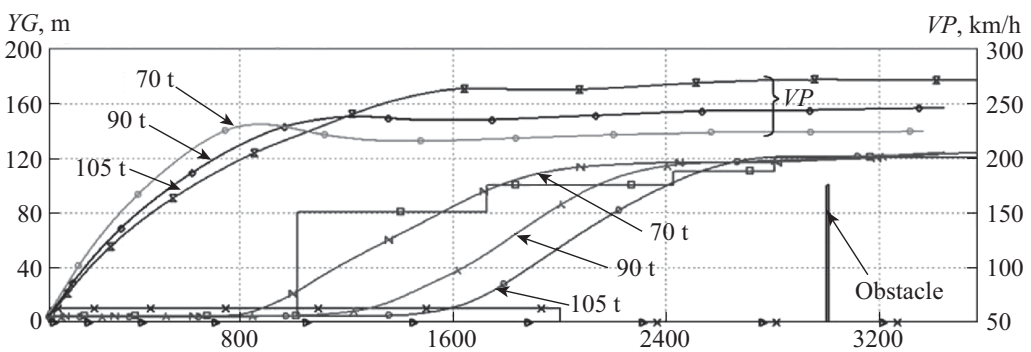

Fig. 3. Transients with the energy control system.

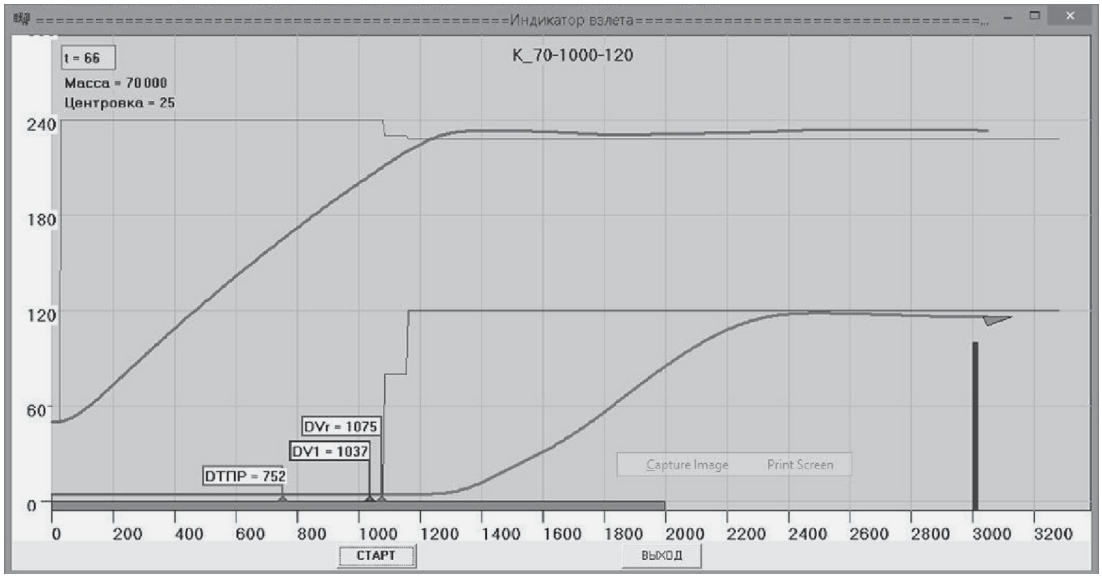

Fig. 4. Cockpit takeoff indicator window.

The simulation was carried out to compare the forecasted decision points for takeoff with the Flight Manual's recommendations for aircraft with different weights (from minimum to maximum) and the location of obstacles with heights of 50–150 m at a distance of 500–3000 m from the runway endpoint. During takeoff, the bench recorded the position of the aircraft on the runway (the coordinate X_{DP}) in which the current energy state was sufficient for a safe takeoff considering the forecasted motion.

Table 1 combines the coordinates of three points for an aircraft with takeoff weights of 70, 90, and 105 tons: the decision points calculated by forecasting ($X_{V_1}^{fore}$), the points of reaching the regulation takeoff speed V_1 factually ($X_{V_1}^{fact}$), and the points of reaching the nosewheel lift-off speed (X_{V_r}).

Clearly, the possibility of overcoming the obstacle, as well as the nosewheel lift-off speed, are forecasted much earlier than the aircraft gains the decision speeds V_1 and V_r prescribed by the Flight Manual.

For bench testing of takeoff modes with information support of the pilot, a prototype of a real-time indicator of aircraft movement on the ground and air segments was implemented. Figure 4 presents the indicator window at the obstacle clearance instant.

The indicator window demonstrates the histories of the set and factual values of the main flight parameters (altitude and speed). The aircraft symbol on the altitude trajectory shows its current position. The runway and obstacle are conditionally depicted as well. The prototype of the indicator successively marks in real time the forecasted distances to the decision point for takeoff (D_{DP}), to the point of reaching the regulation decision speed (DV_1), and to the point of nosewheel lift-off speed (DV_r), including their numerical values.

Table 1. Comparison of forecasted and factual coordinates

Weight, t	V_1, km/h	$X_{V_1}^{fact}$, m	$X_{V_1}^{fore}$, m	V_r, km/h	X_{V_r}, m
70	204	515	153	210	547
90	220	764	508	228	825
106	238	1095	837	245	1203

6. METHOD FOR FORECASTING SAFE BRAKING DISTANCE

Figure 5 shows the landing diagram with the following notations: $x(t)$ is the current position of the aircraft on the runway; D_{brak} is the braking path length; X_{brak} is the end point coordinate; finally, L_{res} is the ground run reserve to the runway endpoint.

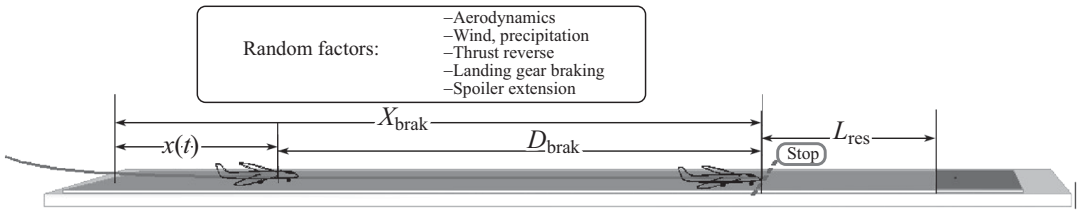

Fig. 5. Landing with braking.

Within the ground segment of the trajectory, during the run after landing or before an aborted takeoff, there may be situations with a risk of overrunning the runway. Under a time deficit, it is necessary to assess the possibility of either emergency braking and stopping within the runway or going around again. We define the braking length as the distance over which the airspeed will be canceled from the current one to some small value ϵ or the taxiing speed.

For the stopping criterion $V(t) \leqslant \epsilon$, the forecasted braking length is given by

$$D_{brak} = \frac{0.5(V^2(t) - \epsilon^2}{gn_x(t)}. \tag{4}$$

According to this estimate of the marginal stopping distance of the aircraft, the pilot may be visually informed of the safe braking distance reserve

$$L_{res} = L_{run} - x(t) - D_{brak}.$$

This information message will help the pilot to make a decision on emergency braking (and in the case of its impossibility, a decision on go-around).

In the process of braking, all forces and conditions change; therefore, the a priori estimates of the aircraft motion on the runway differ from the real ones, containing an inevitable error. Moreover, the current situation forecast is always optimistic since the main braking forces (reverse thrust and aerodynamic drag) relax with decreasing the speed.

To improve the reliability of forecasting, we propose to correct the forecast (4) by introducing a correction Q_{cor} and calculating the corrected braking distance

$$D_{brak\ cor} = Q_{cor} D_{brak}. \tag{5}$$

The highest forecasting errors occur on sections with maximum reverse and with extended spoilers, so the correction coefficients are selected separately for each configuration of the braking devices. These sections are always identifiable, and switching the type of correction is straightforward.

At the beginning of the braking path (the reverse section), the greatest impact on the forecasting errors is exerted by the friction coefficient k_{fric} (which is reported to the board for the landing calculation) and the rolling velocity V (which is bounded by the reverse speed, $V \geqslant V_{rev}$).

The correction coefficient on the reverse section, Q_{rev}, explicitly considers both factors mentioned:

$$Q_{rev} = k_{rev}(k_{fric})k_{rev}(V).$$

The value $k_{rev}(k_{sc})$ was analytically approximated by the polynomials of the second, third, and fourth degrees. The polynomial of the third degree has the form

$$k_{rev}(k_{fric}) = 16.14(k_{fric})^3 - 22.55(k_{fric})^2 + 8.25k_{fric} + 0.716.$$

Despite the differences in the approximating polynomials, the resulting errors varied by no more than 10%.

The empirical dependence of the correction coefficient on speed was found in the form

$$k_{rev}(V) = k_1(k_0 + (1 - k_0))V/V_H,$$

where V_H is the initial braking speed, the coefficient k_1 determines the overall intensity of correction, and the coefficient k_0 changes the degree and sign of correction as the aircraft moves along the runway. The tuning coefficients k_0 and k_1 were determined by minimizing the average forecast error on the reverse section.

On the ground run section with extended spoilers, the correction was achieved by simply scaling the coefficients using the normalized average landing weight $m_{norm=m/90}$:

$$Q_{spoil} = k_i m_{norm}.$$

The values k_i were found by minimizing the error over the entire flight under all braking conditions. After retraction of the spoilers, the correction coefficient was scaled to $Q_{spoil} = 0.8K_i m_{norm}$.

The states of the braking devices and the actions of external factors change at a high rate. Therefore, to smooth out possible high-frequency bursts, all the forecasted values are passed through a damping filter, i.e., an aperiodic link with a tunable time constant Tf_{fore}.

7. STUDIES OF THE BRAKING DISTANCE FORECASTING ALGORITHM

A special simulation bench was created to study the forecasting algorithms. This bench has a set of modes to analyze the forecasting algorithms and to perform their correction and studies as well as developed service tools for setting the experimental conditions and processing and recording the results.

First of all, the bench is used to determine the correction coefficients in terms of the selected optimality criteria (forecasting errors on any trajectory section). The program module of the forecasting algorithms contains a base of settings for the coefficients of the algorithm (5) on a discrete set of braking conditions. To make the coverage of the settings domain continuous, the software includes a module for interpolating the correction coefficients as a function of three variables: $[k_0, k_1, k_i] = INTERPOL[m, k_{fric}, V_{pos}]$.

The service software of the simulation bench includes a module for analyzing the results of statistical tests of the forecasting algorithms. The statistical testing module is configured to analyze the forecasting errors of the stopping point during aircraft braking on the runway. The random disturbances are the variations in aircraft weight and friction coefficient. The distribution law can be assigned as Gaussian or uniform. When displaying the curves on the screen, the experimental distribution function is plotted along with the analytical Gaussian function with the same moments.

Figure 6 shows the experimental distribution functions and the corresponding probability densities of the forecasting errors of the braking distance (ΔD_{brak}) for a 90-ton aircraft from an initial speed of 220 km/h. The analytical approximation of the distribution function by the Gaussian law is plotted on each graph. The mean and the width of the 5% error tolerance are also provided.

According to the graphs, random forecasting errors have distributions close to Gaussian. Small values of the mean and standard deviation indicate high forecasting accuracy, which is achieved by the effective correction of forecasting algorithms.

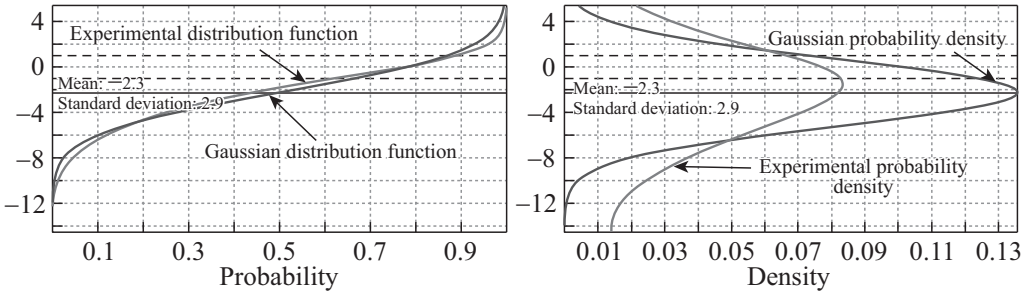

Fig. 6. Distribution functions and probability densities of the forecasting errors of braking distance.

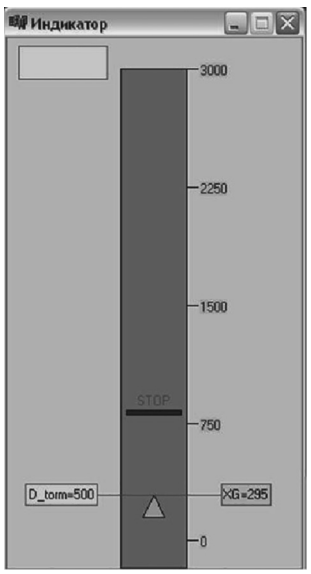

Fig. 7. Braking indicator.

Engine thrust reverse has the strongest impact on the dynamics of the braking process. Increasing the reliability of forecasting on the reverse section is very important: on this section, the speed takes the highest values, increasing the stress load on the pilot. Forecasting errors during the entire braking stage (total errors) and those in the reverse mode only (reverse errors) were investigated and compared. The correction coefficients were determined using two different optimality criteria: by minimizing the errors on the reverse section, min(reverse errors), and by minimizing the errors on the complete braking trajectory, min(total errors).

Table 2 presents the average forecasting errors on the reverse section and on the complete braking trajectory of an aircraft with a landing weight of 90 t, an initial speed of 220 km/h, and friction coefficients of 0.3, 0.5, and 0.75.

These data confirm that the reverse section contributes most to the forecasting error, and optimization in terms of the minimum error on the reverse section also significantly reduces the total error over the entire run.

Table 2. Forecasting errors on the reverse section and complete braking trajectory

Friction coefficient	0.3	0.3	0.5	0.5	0.75	0.75
Optimality criterion	Reverse errors	Total errors	Reverse errors	Total errors	Reverse errors	Total errors
min(reverse errors)	−8.97	−8.94	−0.48	10.27	−0.23	6.03
min(total errors)	−21.35	−3.81	−3.54	−2.0	1.55	0.55

Figure 7 demonstrates the prototype of the braking indicator for information support of the pilot of an aircraft moving in real time along the runway. There are marks of the current position of the aircraft and the forecasted braking endpoint. The numerical value of the aircraft coordinate on the runway and the estimated distance to the stopping point are also shown.

If the forecasted stopping point goes beyond the runway endpoint, it is a signal to go around.

8. CONCLUSIONS

To increase situational awareness of the pilot and reduce stress load, we have developed algorithms for forecasting terminal states during takeoff and landing operations. The algorithms are based on the energy approach to aircraft flight control. This approach allows assessing the current situation and, moreover, the future situation on the forward section of the trajectory, including the air segment of climbing and overcoming a high-rise obstacle. The idea is to inform the pilot of the forecasting results in the form of text, graphic, or audio alerts. In the ground run mode before takeoff, the distance to the decision point on the possibility of safe takeoff and clearance of a high-rise obstacle has been determined. In the braking mode, algorithms for forecasting the distance to the stopping point or to the taxiing speed have been developed. In each mode mentioned, the possibility of safely reaching critical points of the maneuver has been forecasted ahead of their factual occurrence on the trajectory. This gives confidence in fulfilling the flight task in nonstandard or complicated conditions on the runway.

REFERENCES

1. Aviation Accidents and Incidents in the First Quarter of Year 2023. http://old.aviamettelecom.ru.
2. Accidents Statistics. http://www.planecrashinfo.com/cause.
3. Borodkin, S., Volynchuk, A., Ganiev, Sh., et al., Modern Methods of Preventing Aircraft Overrunning the Runway, *Civil Aviation High Technologies*, 2022, vol. 25, no. 2, pp. 1–12.
4. Grebenkin, A. and Burdun, I., Landing under Extreme Conditions: Early Safety Screening by Means of the "Pilot–Automaton–Aircraft–Operating Environment" System Dynamics Model, *Proc. SAE 2019 Aviation Technology Forum*, 2019.
5. Grebenkin, A.V. and Lushnikov, A.A., Human Factor Consideration in the Integration Problems of Manual and Automatic Control of a Trunk Airliner under Complex Multifactor Landing Conditions, *Trudy 2-go Vserossiiskogo foruma s mezhdunarodnym uchastiem "Akademicheskie Zhukovskie chteniya"* (Proc. 2nd All-Russian Forum with International Participation "Academic Readings from Zhukovskii"), Voronezh: Military Training and Research Center of the Air Force, Air Force Academy, 2022, pp. 224–231.
6. Nikiforov, S.P., An Onboard Ground Run Control System as an Effective Means of Improving the Safety of Transport Aircraft Takeoffs, *Aviation Science and Technology*, 2020, nos. 3–4, pp. 47–54.
7. Shevchenko, A., Some Means for Informational Support of Airliner Pilot, *Proc. 5th Int. Conf. on Physics and Control (PhysCon 2011)*, Leon, 2011, pp. 1–5.
8. Kuznetsov, A., Shevchenko, A., and Solonnikov, Ju., The Methods of Forecasting Some Events During the Aircraft Takeoff and Landing, *Proc. 19th IFAC Symposium on Automatic Control in Aerospace (ACA2013)*, Germany, 2013, pp. 183–187.
9. Kurdjukov, A., Nachinkina, G., and Shevtchenko, A., Energy Approach to Flight Control, *Proc. AIAA Conf. on Navigation, Guidance and Control*, AAIA paper no. 98-4211, Boston, 1998.
10. Lambregts, A., Vertical Flight Path and Speed Control Autopilot Design Using Total Energy Principles, AIAA paper no. 83-2239CP, 1983, pp. 559–569.

This paper was recommended for publication by V.M. Glumov, a member of the Editorial Board